Limited impacts of global warming on rockfall activity at low elevations: Insights from two calcareous cliffs from the French Prealps

Robin Mainieri, Nicolas Eckert, Christophe Corona, Jerome Lopez-Saez, Markus Stoffel, Franck Bourrier

Limited impacts of global warming on rockfall activity at low elevations: Insights from two calcareous cliffs from the French Prealps

Robin Mainieri
Univ Grenoble Alpes, Inrae, UR LESSEM, Saint Martin d'Heres, France; Univ Grenoble Alpes, Inrae, UR ETGR, Saint Martin d'Heres, France

Nicolas Eckert
Univ Grenoble Alpes, Inrae, UR ETGR, Saint Martin d'Heres, France

Christophe Corona
GEOLAB, UMR6042 CNRS/Universite Blaise Pascal, Clermont-Ferrand, France

Jerome Lopez-Saez
Institut des Sciences de l'Environnement, Universite de Genève, Geneva, Switzerland

Markus Stoffel
Institut des Sciences de l'Environnement, Universit de Genève, Geneva, Switzerland; Dendrolab.ch, Department of Earth Sciences, University of Geneva, Geneva, Switzerland; Department of Forel for Environmental and Aquatic Sciences, University of Geneva, Geneva, Switzerland

Franck Bourrier
Univ Grenoble Alpes, Inrae, UR ETGR, Saint Martin d'Heres, France

In mountainous regions, global warming will likely affect the frequency and magnitude of geomorphic processes. This is also the case for rockfall, one of the most common mass movements on steep slopes. Rainfall, snowmelt, or freeze-thaw cycles are the main drivers of rockfall activity, rockfall hazards are thus generally thought to become more relevant in a context of climate change. At high elevations, unequivocal relationships have been found between increased rockfall activity, permafrost thawing and global warming. By contrast, below the permafrost limit, studies are scarcer. They mostly rely on short or incomplete rockfall records, and have so far failed to identify climatically induced trends in rockfall records. Here, using a dendrogeomorphic approach, we develop two continuous 60-year long chronologies of rockfall activity in the Vercors and Diois massifs (French Alps); both sites are located clearly below the permafrost limit.

Corresponding author:
Robin Mainieri, Univ Grenoble Alpes, Inrae, UR LESSEM, 2 rue de la papeterie, Saint Martin d'Heres, France. Email: robin.mainieri@inrae.fr

Uncertainties related to the decreasing number of trees available back in time were quantified based on a detailed mapping of trees covering the slope across time. Significant multiple regression models with reconstructed rockfalls as predictors and local changes in climatic conditions since 1959 extracted from the SAFRAN reanalysis dataset as predictants were fitted to investigate the potential impacts of global warming on rockfall activity at both sites. In the Vercors massif, the strong increase in reconstructed rockfall can be ascribed to the recolonization of the forest stand and the over-representation of young trees; changes that are observed should not therefore be ascribed to climatic fluctuations. In the Diois massif, we identify annual precipitation totals and mean temperatures as statistically significant drivers of rockfall activity but no significant increasing trend was identified in the reconstruction. All in all, despite the stringency of our approach, we cannot therefore confirm that rockfall hazard will increase as a result of global warming at our sites.

Keywords
Rockfall, tree-ring reconstruction, climate change, calcareous French Alps

I Introduction

In mountainous environments, mass movements are particularly sensitive to global warming (Gariano and Guzzetti, 2016; Stoffel and Corona, 2014). As air temperatures continue to rise, mass movements are expected to change in terms of their frequency or magnitude as well as in area affected (Hock et al., 2019; Giacona et al., 2021). Among these mass movements, rockfall is a major driver of landscape evolution on steep mountain flanks (Korup, 2006) and thus also presents a serious hazard in mountain regions across the globe (Bovis et al., 1985; Evans and Degraff, 2002). Rockfall involves the independent movement of individual rock fragments that detach from bedrock along new or previously existing discontinuities (e.g., bedding planes, joints, fractures, cleavage, and foliation; Selby, 1993) by creeping, sliding, toppling or falling. Rock fragments typically fall from a cliff, but then proceed downslope by bouncing and flying along ballistic trajectories, or by rolling on talus slopes. Most often, fragmental rockfall involves relatively small volumes (<100 m^3) of isolated rocks or boulders with maximum velocities <30 m.s-1, although there is no well-defined limit of the process in terms of volume or travel velocity (Evans and Hungr, 1993). Rockfall is a sudden phenomenon and difficult to predict in time and space (D'Amato et al., 2016). In rockfallprone areas, slope stability is predominantly controlled by the presence, orientation, and geomechanical properties of discontinuities (Terzaghi, 1962). The actual triggering of rockfall can be ascribed either to external factors (Cruden and Varnes, 1996) such as earthquakes (Keefer, 2002; Malamud et al., 2004; Stoffel et al., 2019), volcanic eruptions (Hale et al., 2009), wave action along shores (Rosser et al., 2005) or anthropogenic activity (Müller, 1964). By contrast, the temporal frequency of rockfall is often modulated by meteorological parameters (Bajni et al., 2021; Delonca et al., 2014; Draebing et al., 2017a, 2017b; D'Amato et al., 2016; Matsuoka, 2019; Nigrelli et al., 2018; Paranunzio et al., 2015, 2016, 2019). The influence of meteorological parameters has been highlighted in various monitoring studies covering a few years up to a decade. Intense rainfall episodes (André, 1997; Berti et al., 2012; Ilinca, 2009; Rapp, 1960), freeze-thaw cycles of interstitial water (Dunlop, 2010; Draebing and Krautblatter, 2019; Hales and Roering, 2007; Ilinca, 2009; Matsuoka and Sakai, 1999; Wieczorek and Jäger, 1996), the thawing of permafrost (Huggel et al., 2012a; Nigrelli et al., 2018; Paranunzio et al., 2016; Stoffel and Huggel, 2012; Sass and Oberlechner, 2012) or rock surface temperature variations (Bakun-Mazor et al., 2013; Collins and Stock, 2016; Collins et al., 2018; Frayssines and Hantz, 2006; Gunzburger et al., 2005; Luckman, 1976) were identified as key triggering mechanisms of rockfall activity in the past. Owing to the sensitivity of the cryosphere to global warming—and the

enhanced warming observed at high altitudes and latitudes as compared to global average (Hock et al., 2019)—causal links have been established between increasing air temperatures and rockfall activity and ascribed to the gradual reduction in the stability of steep bedrock slopes in high mountain regions within the European Alps (Allen and Huggel, 2013; Deline et al., 2012; Huggel, 2009; Ravanel and Deline, 2011; Ravanel et al., 2017). These studies stated that the more rapid succession of cold and extremely warm phases as well as higher rainfall totals would lead to an acceleration of weathering and fragmentation and that mountain regions are thus currently experiencing destabilization. However, even if the events at high elevations can be unequivocally assigned to the current warming trend (Deline, 2009), several flaws exist in past studies: (1) systematically compiled long-term records are largely missing, often imprecise or biased toward more catastrophic events (Moreiras, 2006) while the back analysis of past events is fundamental to assess the role of global warming on rockfall activity (Ravanel and Deline, 2011); (2) research is biased towards glaciated or permafrost areas, whereas most rockfall threatening infrastructure occur on slopes located far below the permafrost limit (Sass and Oberlechner, 2012) (Table 1).

At lower elevations, Gruner (2004) and Sass and Oberlechner (2012) found an increase in rockfall frequency is neither recognizable at present nor to be expected in the near future. The fact that results are different between high and low-elevation sites and that they remain scarce outside cryospheric environments clearly highlights the necessity for analyses at lower elevations and at the local/regional rather than at larger scales. On forested slopes, falling rocks and boulders interact with forest stands (Dorren et al., 2007). Rocks impacting trees leave characteristic scars on their trunks and growth disturbances (GD) in the tree-ring series. GDs have been proven to be reliable, accurate and precise indicators of past rockfall activity and that past rockfall can be reconstructed with dendrogeomorphic techniques in space and time (Alestalo, 1971; Stahle et al., 2003; Stoffel et al., 2005b; Stoffel and Corona, 2014). Tree-ring reconstructions have been used successfully to derive past rockfall frequency (Morel et al., 2015; Mainieri et al., 2019; Stoffel and Perret, 2006; Trappmann et al., 2013) or to document source areas or trajectories (Stoffel et al., 2006; Trappmann et al., 2013). Yet, with the exception of Perret et al. (2006), Silhán et al. (2011) and Zielonka and

Table 1. Synthesis of studies related to the impacts of climate change on rockfall activity in Alps.

Author	Date	Location	Elevation (m a.s.l)	Time-period	Nb of rockfall events
Noetzli et al.	2003	Swiss, Italian, and German Alps	>2300	1717–2002	20
Gruner	2004	North side of the Alps of Switzerland	\	1500–2000	800
Perret et al.	2006	Schwarzenberg (Swiss Alps)	1250	1724–2002	301
Schneuwly and Stoffel	2008	Saas Balen (Swiss Alps)	1610	1975–2006	154
Ravanel and Deline	2008	Mont blanc massif	>3000	1905–2005	8
Ravanel et al.	2010	Mont blanc massif	>2700	2007–2008	66
Ravanel and Deline	2011	Mont blanc massif	3100	1947–2010	42
Huggel et al	2012	Mont blanc and central Alps	>2000	1900–2010	52
Fischer et al.	2012	Central Alps	>2000	1900–2007	56
Sass and Oberlechner	2012	Austria	< Permarfrost limit	1900–2010	252
Allen and Huggel	2013	Swiss Alps and Mont blanc massif	>2000	1987–2011	41
Ravanel et al.	2017	Mont-Blanc massif	>2600	2003; 2005	153; 78
Viani et al.	2020	Western Italian Alps	>2700	1956–2019	10

Wronska-Wałach (2019), tree-ring reconstructions were only rarely compared with instrumental weather data series with the aim to assess the impact of global warming on rockfall activity at sites located below the permafrost limit. This lack of studies can be explained partly by the almost systematic increasing trend observed in rockfall activity toward the recent past which is related to (1) the continuous reduction in the number of trees available for analysis and the diameter of exposed trees as one goes back in time (Stoffel et al., 2005b) and (2) the associated decline of potentially recordable GDs (Trappmann and Stoffel, 2013). Here we aim to quantify potential impacts of climate variations on rockfall activity at two calcareous cliffs in the French Prealps located outside periglacial environments. To account for the biases and related limitations mentioned above, we used the tree-ring based rockfall reconstructions developed by Mainieri et al. (2020a, 2021) in which reconstruction uncertainties have been precisely quantified over time. The debiased reconstructions were then contrasted with climate series from highly resolved meteorological reanalyzes (Durand et al., 2009b) using different empirical and model-based statistical approaches. This procedure allows highlighting the weak control of changing climatic conditions on rockfall at both sites, and, more widely, to discuss the potential impact of the ongoing warming on rockfall frequency at low elevation sites outside ice-dominated environments.

1.1 Study sites

The two study sites are located in the Vercors (Saint-Guillaume) and Diois (Valdrôme) massifs (French Alps) and are 60 km apart from each other (Figure 1(a)). Saint-Guillaume is located on the northern slope of the Pale mountain, close to the "Rocher du Bouchet" (44°56′18″*N*, 5°35′11″E). Here, rockfall is released from a 90-m high, north-east-facing cliff (1450–1540 m asl) consisting of subhorizontally bedded Jurassic limestone (Tithonian) with narrow orthogonal joints. This structure favors the release of rock fragments with volumes that are generally smaller than a few m^3. In the transit area of rockfall (1380–1490 m asl), Quaternary scree is characterized by a convex-concave slope profile (26–46°, ∅ 38°) with a marked longitudinal sorting of debris with volumes of a few dm^3 at the apex to a few m^3 in the lower portion of the slope. The slope is covered by a mixed forest stand (see Mainieri et al., 2021 for a detailed description). Even though evidence of past logging (stumps) could not be found at the site, we cannot rule out the possibility that some limited silvicutural interventions did occur at the slope over the course of the last century. Rockfall is the predominant cause of damage on tree stems yet snow avalanches of limited extent cannot be excluded in the upper part of the slope. Valdrôme (Figure 1(c)) is located on the west-facing slope of the Arcs mountain, Diois massif (44°32′90″ *N*, 5°33′76″ E, 790–880 m asl, Figure 1(a)). Here, rockfall is triggered from several release areas located within a roughly 40-m high, west-facing cliff (890–930 m asl). This Jurassic (Thitonian) cliff is composed of sublithographic limestone with a content of marls (5–6%) characterized by narrow jointing, subhorizontal bedding and subvertical orthogonal joints, favoring fragmentation and the release of small rock fragments with volumes ranging from a few cm^3 to a few dm^3. In the field, the presence of recent scars on the cliff and fresh blocks deposited on the slope testify the existence of current rockfall activity at the site. The talus slope, with angles varying from 35 to 45° (∅ 40°), is characterized by a marked longitudinal sorting of clasts with volumes of a few cm^3 at the apex to a few dm^3 in the distal segment. It is covered by a dense (1800 trees.ha^{-1}) monospecific forest stand composed of *Pinus nigra* (Austrian black pine) planted at the beginning of the 20th century (1902) by the French forest service. Field observations confirm that rockfall is the dominant process on the studied slope (see Mainieri et al., 2019 for a detailed description of the study site). According to meteorological re-analyses data provided by SAFRAN (Durand et al., 2009b; Vernay et al., 2019), total precipitation (1958–2017) amounts to 951 mm (±201 mm) and 1022 mm (±195 mm) on average at Saint-Guillaume and Valdrôme, respectively. The driest season is winter (96 ± 55 mm, 182 ± 172 mm at Saint-Guillaume and Valdrôme), whereas wetter conditions prevail in autumn (330 ± 131 mm, 339 ±143 mm). At Saint-Guillaume, mean annual,

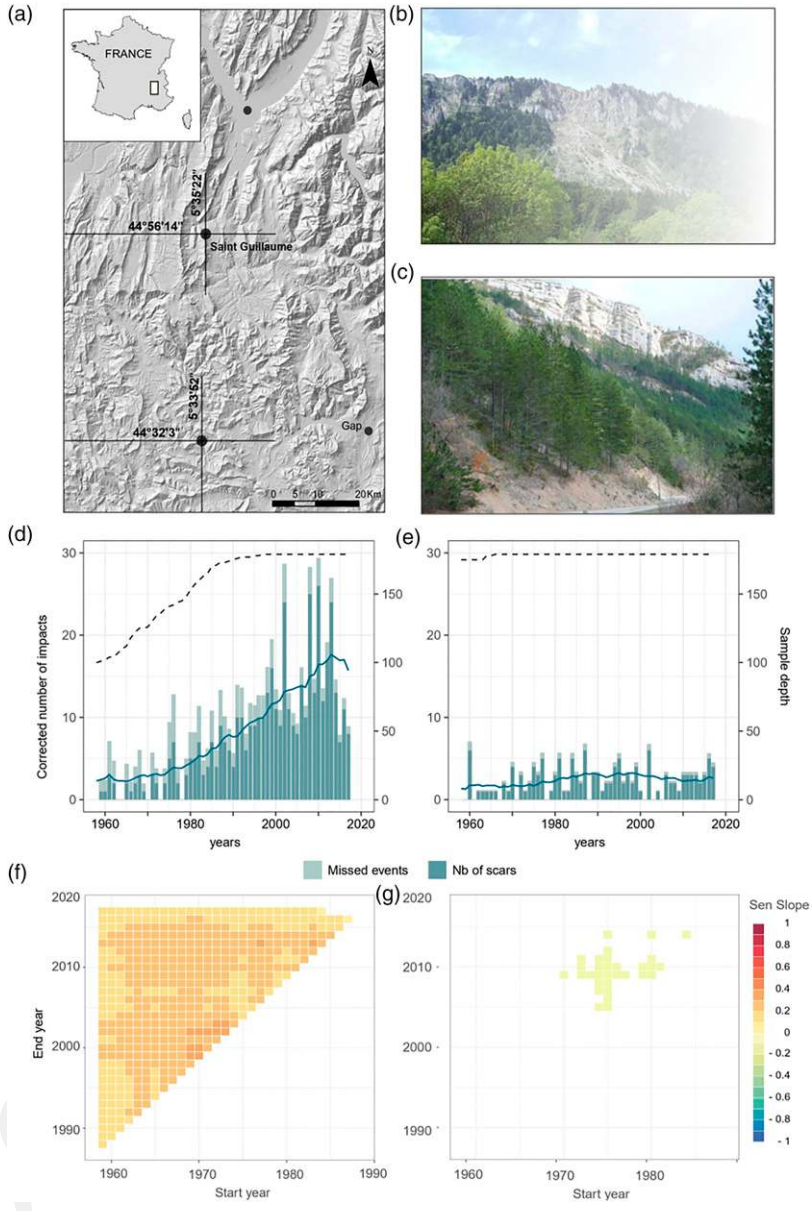

Figure 1. The Rocher du Bouchet (b) and Valdrˆome (c) sites are located in the Vercors and Diois massifs massif (a). At both sites (d, e), fluctuations of rockfall activity were reconstructed from tree-ring analyses. Linear monotonic trends in the reconstructions were quantified using the Theil-Sen slope (f, g) and their significance ($p < 0.05$) has been tested using a Mann-Kendall (MK) test. For each reconstruction, the MK test was computed over the 1959–2017 period covered by meteorological series, for moving time windows with length varying from 30 to 59 years. Starting years (x-axis) range between 1959 and 1988, ending years (y-axis) between 1988 and 2017. For interpretation of the references to colours in this figure legend, refer to the online version of this article.

winter and spring temperatures average 5.7 (±0.7°C), 1.1 (±1.2°C), 4.1 (±0.9°C), respectively (Figure 2(c)). Due to marked Mediterranean influence, warmer conditions are observed at Valdrôme with mean annual, winter and spring temperatures averaging 10.2 (±0.6°C), 1.1 (±1.1°C), and 8.2 (±0.9°C), respectively (Figure 3(c)). On average, 78 (±12, Saint-Guillaume) and 90 (±14, Valdrôme) freeze-thaw cycles occurred

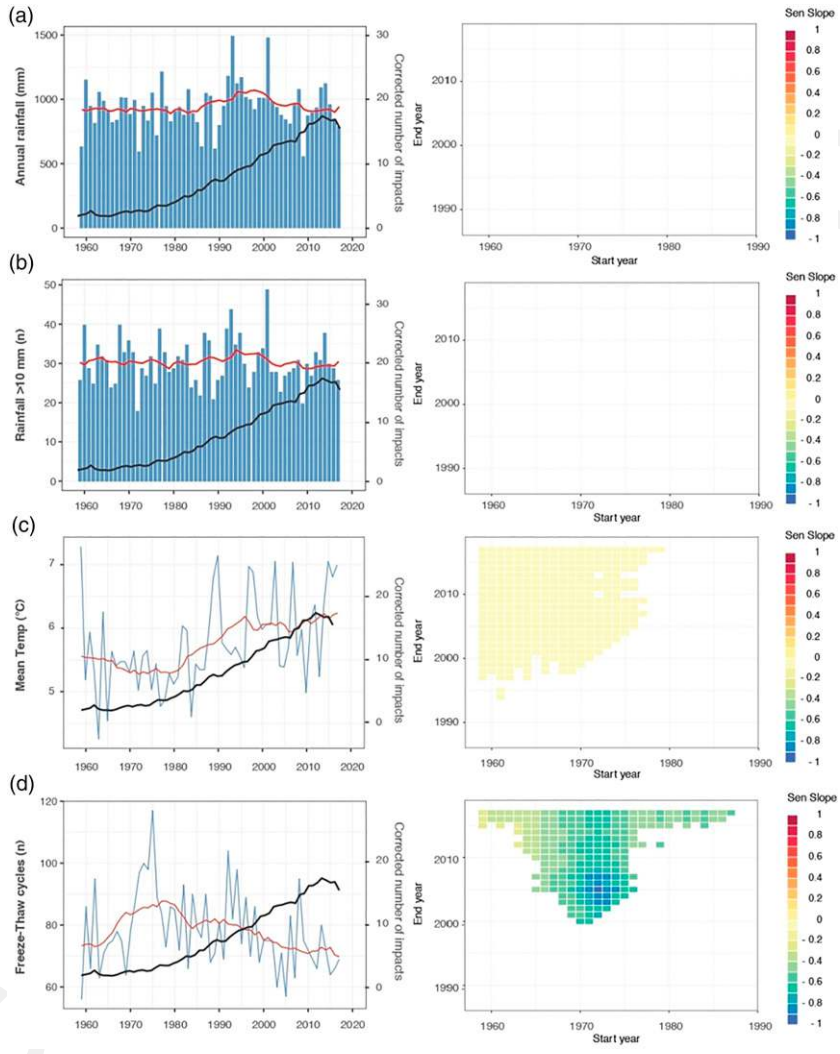

Figure 2. Linear monotonic trends (Theil-Sen slope, right panel) detected in annual records (left panel) of (a) rainfall (in mm), (b) number of rainfall events >10 mm (PR10), (c) mean temperature and (d) number of days with freeze-thaw cycles at Saint-Guillaume. The annual values (blue bars and lines) were computed from October (n-1) prior to tree-ring formation to September (n). A 15-years running average has been used to emphasize decadal fluctuations of climate (red line). Black curves represent decadal fluctuations of reconstructed rockfall activity. The significance of the trends ($p < 0.05$) has been tested using the Mann-Kendall test. For each climatic parameter, the MK test was computed over the 1959–2017 period, for moving time windows with length varying from 30 to 59 years. Starting years (x-axis) range between 1959 and 1988, ending years (y-axis) between 1988 and 2017. For interpretation of the references to colours in this figure legend, refer to the online version of this article.

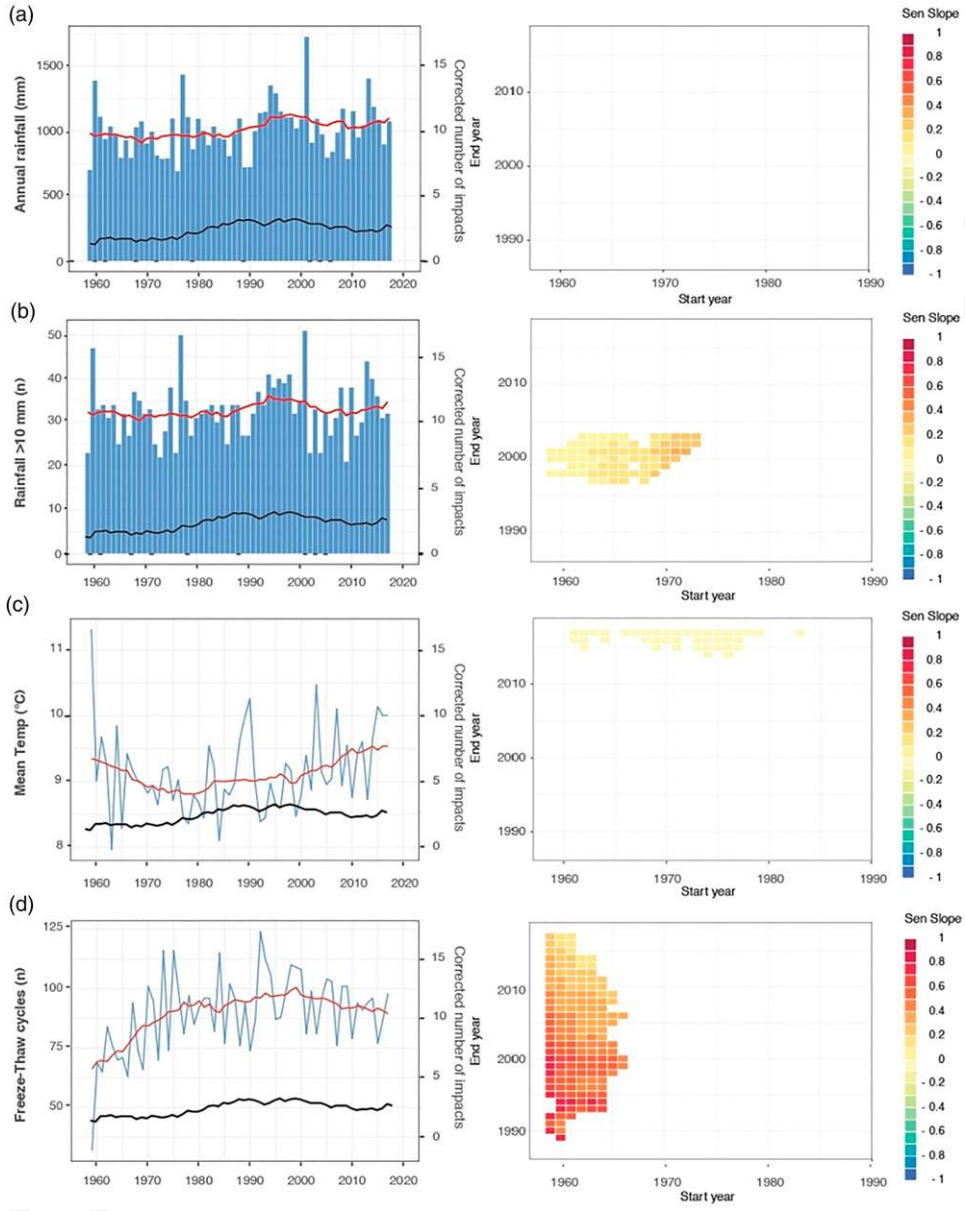

Figure 3. Linear monotonic trends (Theil-Sen slope, right panel) detected in annual records (left panel) of (a) rainfall (in mm), (b) number of rainfall events >10 mm (PR10), (c) mean temperature and (d) number of days with freeze-thaw cycles at Valdrôme. The annual values (blue bars and lines) were computed from October (*n*-1) prior to tree-ring formation to September (n). A 15-years running average has been used to emphasize decadal fluctuations of climate (red line). Black curves represent decadal fluctuations of reconstructed rockfall activity. The significance of the trends ($p < 0.05$) has been tested using the Mann-Kendall test. For each climatic parameter, the MK test was computed over the 1959–2017 period, for moving time windows with length varying from 30 to 59 years. Starting years (*x*-axis) range between 1959 and 1988, ending years (*y*-axis) between 1988 and 2017. For interpretation of the references to colours in this figure legend, refer to the online version of this article.

every year at the study sites between 1959 and 2017, mainly during winter and spring (85%).

II Methods

2.1 Tree-ring reconstructions

The dendrogeomorphic records used here are from Mainieri et al. (2020a) (Valdrôme) and Mainieri et al. (2021) (Saint-Guillaume). The sample strategies and the analyses extensively described in both publications are synthesized hereafter. At both study sites, virtually all trees show visible growth anomalies on the stem surface resulting from past rockfall, predominantly in the form of injuries. As scars represent the most accurate and reliable growth disturbance (GD) to date past rockfalls in tree-ring records Stoffel et al. (2013), we actively searched for visible stem wounds at the study site. To assess spatial and temporal patterns of past rockfall activity, trees with a diameter at breast height (DBH) > 4 cm were systematically mapped on 1 ha plots (110 × 90 and 110 × 115 m at Saint-Guillaume and Valdrôme, respectively). The position of each tree (n = 793) at Saint-Guillaume, n = 1479 at Valdrôme) was determined with a theodolite measuring azimuth (compass), distance (Vertex), and slope (inclinometer). All trees were positioned in a geographical information system (GIS) as geo-objects. In order to estimate the likelihood that a rockfall does not impact any of the sampled tree trunks, we used the Conditional Impact Probability (CIP; Favillier et al., 2017; Moya et al., 2010; Trappmann et al., 2013) approach as it quantifies the range covered by all sampled trees at any given year and therefore allows to take account of changing tree sizes and tree numbers. Based on our systematic inventory, we equally use the CIP to optimize our sampling strategy. Accordingly, trees located upslope, that represent the first barrier to rockfall, were sampled preferentially while those located in the direct fall line of other trees and that would thus protect each other were systematically ignored. The annual rockfall rate (RR) was computed as the ratio between the number of growth disturbances dated and the CIP for year t (see Mainieri et al., 2020a, 2021). Based on our improved strategy, an increment core (max. 40 × 0.5 cm) was sampled at the lateral edges of each visible scars in the overgrowing callus tissue (Larson, 1994; Sachs, 1991) for each selected tree. In addition, based on observed bounce heights—which usually remain below 2 m on the plot—three additional increment cores were systematically extracted, in the fall line direction, at heights of 0.5, 1.0, and 1.5 m, in order to increase the potentiality to retrieve old healed impacts.

For the period 1959–2017 covered both by the tree-ring records and the meteorological series, our dataset contains 179 tree-ring series from various species of conifers (*Picea abies, Abies alba*) and broadleaved (mainly *Fagus sylvatica*) at Saint-Guillaume and from *P. nigra* trees at Valdrôme. In total, 446 (Saint-Guillaume) and 136 (Valdrôme) GDs were dated in the tree-ring series. Over this period, the CIP continuously increased from 0.41 to 0.81 at Saint-Guillaume and remains more stable (0.85–0.88) at Valdrôme. At Saint-Guillaume, the corrected annual rockfall frequency increased from 5.5 GD.yr^{-1} to 14.5 GD.yr^{-1} for the periods 1959–1988 and 1989–2017, respectively (Figure 1(d)). At Valdrôme, the mean corrected number of impacts only slightly increased between the periods 1959–1988 (2.4 GD.yr^{-1}) and 1989–2017 (2.8 GD.yr^{-1}). The decades 19,601,969 (1.4 GD.yr^{-1}) and 2000–2009 (1.6 GD.yr^{-1}) are characterized by the lowest frequencies of impacts (Figure 1(e)).

To detect potential trends in rockfall (and meteorological) time series, we applied the non-parametric Mann-Kendall (MK) test (Helsel et al., 1992). This rank-based procedure is especially suitable for non-normally distributed data and is robust against outliers and data gaps. The MK test yields a trend test statistic that allows rejection of the null hypothesis at a certain significance level (Birsan et al., 2005). The slope of trends significant at the 95% level of the MK test was estimated using the Theil-Sen method, which is suitable for nearly linear trends and has been shown to be mostly unaffected by non-normal data and outliers (Helsel et al., 1992).

According to the MK test computed over the 1959–2017 period, a significant linear monotonic increasing trend (significant at $p < 0.05$) exists at

Saint-Guillaume for most of the considered time periods prior to 1987 (Figure 1(f)). Conversely, at Valdrôme, no significant trend is detected in the reconstruction over the same period (Figure 1(g)).

2.2 Meteorological data from the SAFRAN reanalysis

At the study sites, meteorological time series were obtained from the SAFRAN re-analyses downscaling and surface analysis system (Durand et al., 2009b). This system performs an objective analysis of weather data available from various observation networks (including radar and satellite data) to provide freely available, continuous time series of meteorological variables at hourly resolution, for elevation steps of 300 m, different slope aspects and angles within massifs, and therefore for horizontally and climatologically homogeneous regions (Lafaysse et al., 2013; Vernay et al., 2019). In a preliminary step, we checked correlations (19,662,019) between mean temperature and precipitation totals from SAFRAN, aggregated on a monthly basis, and the records available from meteorological stations (Monestier-de-Clermont, 44°55′18″ *N*, 5°38′15″ E, 806 m asl; Valdrôme, 44°30′19″ *N*, 5°34′36″ E, 786 m asl) next to the study sites (3 and 4 km east from Saint-Guillaume and Valdrôme, respectively). All correlations are significant at $p < 0.05$ (Table 2), confirming that reanalayses can be confidently used to infer potential linkages with rockfall activity at both sites.

Delonca et al. (2014) and D'Amato et al. (2016) synthesize the current understanding of physical processes related to meteorological parameters that are susceptible to trigger rockfall. In calcareous regions, amongst the most frequent triggers cited in literature are rainfall duration and intensities that increase pressure in rock joints, freeze-thaw cycles through wedging and loss of cohesion as well as temperature variations through thermal stresses which propagate cracks. To be able to investigate the role of meteorological variables in controlling/promoting these processes, 10-days to annual series (i.e., 360 days, or 36 10-day series) of (1) precipitation sums, (2) number of rainfall events above 10 and 20 mm day-1, (3) mean variations of air temperature as well as (4) the absolute number of freeze-thaw cycles (defined as the number of days in which Tmax>0°C and Tmin<0°C) were extracted from the SAFRAN database for the period 1959–2017.

Table 2. Pearson correlation coefficient between mean temperature (Tmean) and precipitation totals (PR) from SAFRAN reanalyzes, aggregated on a monthly basis and the records available from meteorological stations (Monestier-de-Clermont and Valdrôme) located at the vicinity of both study sites.

	Valdrôme		Saint-Guillaume	
Month	Tmean	PR	Tmean	PR
January	0.92	0.87	0.87	0.66
February	0.95	0.86	0.95	0.69
March	0.91	0.92	0.95	0.62
April	0.86	0.95	0.93	0.73
May	0.9	0.9	0.93	0.80
June	0.91	0.84	0.91	0.83
July	0.89	0.76	0.90	0.88
August	0.88	0.8	0.89	0.80
September	0.88	0.94	0.92	0.95
October	0.91	0.97	0.93	0.91
November	0.91	0.96	0.88	0.73
December	0.87	0.84	0.86	0.62

All values are significant at $p < 0.05$

2.3 Linear models and stepwise regressions

Relationships between rockfall activity and meteorological parameters were assessed at the annual (considered from October (*n*-1) prior to the growing season to September n) and at the decadal scales. At the later timescale, rockfall reconstructions and meteorological series were smoothed using 15-years moving averages so as to investigate (1) potential relationships between rockfall activity and climatic fluctuations at decadal time scale and to account for (ii) a time lag may exist between the impact of climatic forcing and the triggering (e.g., Crozier, 2010; Haeberli and Beniston, 1998; Huggel et al., 2012b; Savi et al., 2021). To account for the decreasing number of existing trees back in time, tree-ring reconstructions (RR) were debiased as follows:

$$RR - Std_t = \left(RR_t/SS_t\right) \Big/ \left(\sum_{t=1}^{nyear} SSt/nyear\right) \quad (1)$$

where RR-Std represent the detrended rockfall chronology, SS_t the sample size at year t and *n year* the number of years covered by both meteorological series and rockfall reconstructions (59 in our case). In a first step, (1) Pearson correlation coefficients were calculated between raw as well as detrended (smoothed) rockfall reconstructions and each of the (smoothed) meteorological series mentioned in the previous paragraph. The statistical significance of results was tested with a one-tailed t-test at a significance level $\alpha = 0.05$.

In a second step, for 15-years smoothed series, we developed stepwise regression procedures to determine which combination of independent variables affect rockfall activity at the two study sites. Starting from an initial null model with no covariates and then comparing the explanatory power of incrementally larger and smaller models, we then used a stepwise procedure to combine forward selection and backward elimination of variables using the Akaike Information Criteria (AIC) as metric to compare the relative quality of different models. Forward selection tests all the variables retained at step 2, one by one, and includes them in the final selection if they are statistically significant based on the *p* value of the t-statistics, whereas backward elimination starts with all candidate variables and tests them one by one for statistical significance, deleting those that are not significant based on the *p*-value of the t-statistics. Stepwise regression procedures were developed using the smoothed RR and RR-std reconstructions as explained variables while years, sample size and the smoothed meteorological series were retained as explanatory covariables.

Performance was evaluated with several indicators such as AIC, its small-sample corrected version Akaike Information Criteria corrected (AICc) and the adjusted R^2 determination coefficient. For all the models retained by the stepwise regression, normality of the residuals was tested with the classical Shapiro-Wilks and Anderson-Darling tests. Eventually, we tested the significance of retained models with a F-test within a variance decomposition setting that compares the model with retained covariates with a null model with no covariates.

III Results

3.1 Evolution of climatic conditions at both sites since 1959

According to the Mann-Kendall test, no significant trend can be found in annual rainfall series over the 1959–2017 period for moving time windows with length varying from 30 to 59 years at the study sites (Figures 2(a) and 3(a)). Above average annual precipitation totals were observed at Saint-Guillaume (1070 mm) and Valdrôme (1104 mm) between 1990 and 1999 while driest conditions occurred between 1980 and 1989 (887 mm at Saint-Guillaume and 950 mm at Valdrôme, respectively). Similarly, no trend was observed in the number of rainfall events >10 mm at Saint-Guillaume (Figure 2(b)) whereas a significant, albeit limited increase (<0.4 $mm.yr^{-1}$) was observed in the Diois massif for time periods starting between 1959 and 1973 and ending in 2003 (Figure 3(b)). Mean annual temperatures increased sharply between 1980 and 1995 in the Vercors massif (Figure 2(c)). Consequently, average temperatures computed for the period 1959–1980 (5.4°C) and 1995–2017 (6.2°C) differ significantly. Warming is less pronounced at Valdrôme (Figure 3(c)) with average temperature increasing from 9 (1951–1980) to 9.3°C (1995–2017). Finally, and more interestingly, the number of freeze-thaw cycles significantly decreased between 1959 and 2017 at Saint-Guillaume with the sharpest decline observed between 1973 and 2003 (−1 cycle per year, on average, Figure 2(d)). By contrast, at Valdrôme, the mean number of freeze-thaw cycles computed between 1960 and 1969 (73 on average) was significantly lower than during the subsequent periods (95 cycles on average between 2000 and 2009) and no significant trend was observed in the records when Mann-Kendall tests were computed for time windows starting after 1967 (Figure 3(d)).

3.2 Correlation between rockfall activity and climatic variables

The matrix in Table 3 synthesizes correlations between the rockfall reconstructions (RR, RR-std), meteorological variables as well as years and sample size considered as potential explanatory variables for rockfall fluctuations. The 0.99 (Saint-Guillaume) and 1.00 (Valdrôme) correlation coefficients computed between RR and RR-std demonstrate the limited impact of the standardization on the shape of rockfall chronologies at both sites. The significant correlation computed between rockfall activity, and sample size (r = 0.68) at Saint-Guillaume in addition reveals that the trend in rockfall activity which we previously evidenced in the reconstruction (based on the Mann-Kendall analysis) can be explained partly by the increasing number of trees over the period analyzed (1959–2017). We do not observe such a trend at Valdrôme, where correlations between rockfall activity, years and sample size are insignificant.

Irrespective of the study site analyzed, we do not find any significant correlation between the reconstructed rockfall activity and meteorological variables. Comparable yet not significant correlation are computed between rockfall activity and annual rainfall at Saint-Guillaume (r = 0.12) and Valdrôme (r = 0.15). Regarding mean temperature, inverse correlations are obtained at Saint-Guillaume and Valdrôme with r = 0.18 and r = −0.24, respectively.

Correlations between smoothed series are presented in Table 4. Except for years and sample size, retained at annual resolution, rockfall records and the meteorological variables were smoothed using a 15-years running mean. The positive and highly significant correlation coefficients computed between the smoothed tree-ring records and the "years" variable reveal that rockfall activity decreases at both sites as one goes back in time. Mean temperatures (r = 0.64), annual rainfall (r = 0.49) and—to a lesser extent—the annual number of

Table 3. Correlation matrices (Pearson coefficient) computed for the rockfall reconstruction (RR-std, RR), meteorological parameters (PR: annual rainfall total, PR10: annual number of rainfall events >10 mm, Tmean: mean annual temperature, FT cycles: annual number of freeze-thaw cycles), and additional variables (year, SS: sample size).

Saint-Guillaume	RR	RR-Std	PR	PR10	Tmean	FT cycles	Years	SS
RR	**1.00**	**0.99**	0.12	−0.01	0.18	0.00	**0.73**	**0.68**
RR-std		**1.00**	0.09	−0.02	0.15	0.04	**0.65**	**0.59**
PR			**1.00**	**0.88**	−0.14	0.10	0.10	0.14
PR10				**1.00**	−0.16	0.04	−0.03	0.00
Tmean					**1.00**	**−0.39**	**0.43**	**0.36**
FT cycles						**1.00**	−0.23	−0.09
Years							**1.00**	**0.91**
SS								**1.00**
Valdrôme	**RR**	**RR-std**	**PR**	**PR10**	**Tmean**	**FT cycles**	**Years**	**SS**
RR	**1.00**	**1.00**	0.15	0.17	−0.24	0.24	0.20	0.14
RR-std		**1.00**	0.16	0.17	−0.24	0.23	0.20	0.13
PR			**1.00**	**0.89**	−0.22	0.06	0.23	−0.01
PR10				**1.00**	−0.18	0.01	0.11	−0.02
Tmean					**1.00**	**−0.45**	0.18	−0.15
FT cycles						**1.00**	**0.40**	**0.49**
Years							**1.00**	**0.52**
SS								**1.00**

Annual values were computed between October (n-1) prior to tree-ring formation and September (n). The bold values differ from 0 at a p < 0.05 significance level.

Table 4. Correlation matrices (Pearson coefficient) computed for the rockfall reconstruction (RR-std, RR), meteorological parameters (PR: annual rainfall total, PR10: annual number of rainfall events >10 mm, Tmean: mean annual temperature, FT cycles: annual number of freeze-thaw cycles), and additional variables (year, SS: sample size).

Saint-Guillaume	RR	RR-Std	PR	PR10	Tmean	FT cycles	Years	SS
RR	**1.00**	**1.00**	**0.49**	0.03	**0.64**	**−0.37**	**0.96**	**0.90**
RR-std		**1.00**	**0.46**	0.00	**0.65**	**−0.40**	**0.95**	**0.88**
PR			**1.00**	**0.85**	0.04	**0.30**	**0.38**	**0.61**
PR10				**1.00**	−0.21	**0.42**	−0.08	0.19
Tmean					**1.00**	**−84**	**0.65**	**0.44**
FT cycles						**1.00**	**−0.33**	−0.04
Years							**1.00**	**0.91**
SS								**1.00**
Valdrôme	**RR**	**RR-std**	**PR**	**PR10**	**Tmean**	**FT cycles**	**Years**	**SS**
RR	**1.00**	**1.00**	**0.61**	**0.61**	**−0.32**	**0.82**	**0.69**	**0.70**
RR-std		**1.00**	**0.60**	**0.60**	**−0.32**	**0.82**	**0.69**	**0.70**
PR			**1.00**	**0.92**	−0.14	**0.76**	**0.85**	0.57
PR10				**1.00**	**−0.38**	**0.78**	**0.64**	**0.61**
Tmean					**1.00**	**−0.62**	0.11	**−0.69**
FT cycles						**1.00**	**0.70**	**0.89**
Years							**1.00**	**0.52**
SS								**1.00**

Rockfall and meteorological series have been smoothed using a 15-years moving average, Years and Sample Size have been retained with an annual resolution. The bold values differ from 0 at a $p < 0.05$ significance level.

freeze-thaw cycles (−0.37) are significantly ($p < 0.05$) correlated with the smoothed tree-ring reconstruction at Saint-Guillaume. The annual number of intense rainfall events (<10 mm) do not appear as a significant predictor of rockfall activity ($r = 0.03$). At Valdrôme, correlations differ insofar as—at the decadal scale—the annual number of freeze-thaw cycles ($r = 0.82$), annual precipitation ($r = 0.61$) and intense rainfalls ($r = 0.61$) appear to be the main drivers of rockfall activity whereas and conversely to Saint-Guillaume, a negative correlation is computed ($r = -0.32$, $p < 0.05$) between rockfall activity and mean temperature.

Based on the correlation matrices presented in Table 4, five (SG1-SG5, Saint-Guillaume) and eight (VD1VD8, Valdrôme) multiple regression models were successively fitted using smoothed (detrended) rockfall reconstructions (RR, RR-std) as predictands; and smoothed climatic series, years and sample size (unfiltered) as combinations of regressors. All models presented here are significant at $p < .0001$ (Tables 5 and 6) and, for most of them, normality of residuals cannot be rejected at the 0.05% significance level. Normality of residuals cannot be rejected at $p < 0.05$ for most of the selected models, namely VD3-VD8 and SG1-SG2, and for other models, p-values are just above the significance level, which suggests that, for all models, dispersion of residuals around model prodictions is reasonable. More importantly, all retained models are significant at $p < 0.0001$ from the perspective of the F-test, so that they all convey meaningful information regarding the drivers of interannual variability in rockfall activity.

At Saint-Guillaume, comparison between SG1 and SG2 reveals that the detrended (RR) and non-detrended (RR-std) rockfall chronologies portray comparable climatic signal (Table 5). Except for SG5, mean temperature (in combination with precipitation totals, sample size, or years) appears as the common regressor in all models, thus confirming the positive and significant correlation computed

Table 5. Multiple regression analyses (SG1-SG5) computed between the rockfall reconstructions (RR-std, RR) from Saint-Guillaume used as predictands, meteorological parameters (PR: annual rainfall total, PR10: annual number of rainfall events >10 mm, Tmean: mean annual temperature, FT cycles: annual number of freeze-thaw cycles) years and sample size (SS) used as predictors.

Model	Explained variable	Initial variables	Selected predictands	Coefficients		R^2	AIC	AICc	mod. *p*-value	Shapiro-Wilks	Anderson-Darling
SG1	RR	PR. Tmean	PR, Tmean	Constant	−73.068	0.63	137.566	137.937	<0.0001	0.547	0.872
				PR	0.036						
				Tmean	8.351						
SG2	RR-std	PR, Tmean	PR, Tmean	Constant	−52.245	0.60	106.499	106.869	<0.0001	0.393	0.519
				PR	0.026						
				Tmean	6.376						
SG3	RR	PR, Tmean, years	PR, Tmean, years	Constant	−493.094	0.94	29.749	30.315	<0.0001	0.000	<0.0001
				Years	0.242						
				PR	0.014						
				Tmean	1.408						
SG4	RR	PR, Tmean, SS	Tmean, SS	Constant	−37.180	0.90	63.258	63.628	<0.0001	0.020	0.015
				Tmean	4.121						
				SS	0.145						
SG5	RR	PR, FT cycles, years	PR, FT cycles, years	Constant	−472.990	0.96	14.724	15.290	<0.0001	0.015	0.027
				PR	0.018						
				FT cycles	−0.138						
				Years	0.240						

Rockfall and meteorological series have been smoothed using a 15-years moving average, Years and Sample Size have been retained with an annual resolution. Selected predictands correspond to initial variables retained in each model after the stepwise selection.

Table 6. Multiple regression analyses (VD1-VD8) computed between the rockfall reconstructions (RR-std, RR) from Valdrôme used as predictands, meteorological parameters (PR: annual rainfall total, PR10: annual number of rainfall events>10 mm, Tmean: mean annual temperature, FT cycles: annual number of freeze-thaw cycles) years and sample size(SS) used as predictors.

Model	Explained variable	Initial variables	Selected variables	Coefficients		R^2	AIC	AICc	mod. p-value	Shapiro-Wilks	Anderson-Darling
VD1	RR	PR, Tmean	PR, Tmean	Constant	1.304	0.42	−67.41	−67.040	0.0001	0.004	0.001
				PR	0.006						
				Tmean	−0.496						
VD2	RR-std	PR, Tmean	PR, Tmean	Constant	1.243	0.42	−68.104	−67.734	0.0001	0.004	0.001
				PR	0.006						
				Tmean	−0.483						
VD3	RR	PR, Tmean, years	PR, Tmean, Years	Constant	−70.822	0.67	−97.669	−97.103	0.0001	0.496	0.551
				PR	−0.004						
				Tmean	−0.983						
				Years	0.043						
VD4	RR	PR, Tmean, SS	PR, SS	Constant	−60.44	0.56	−82.932	−82.562	0.0001	0.166	0.115
				PR	0.003						
				SS	0.335						
VD5	RR	PR, FT cycles	FT cycles	Constant	−1.89	0.67	−102.252	−102.034	0.0001	0.029	0.133
				FT cycles	0.05						
VD6	RR	FT cycles, years	FT cycles, years	Constant	−20.357	0.69	−105.429	−105.059	0.0001	0.660	0.814
				FT cycles	0.04						
				Years	0.01						
VD7	RR	FT cycles, SS	FT cycles	Constant	−1.89	0.67	−102.252	−102.034	0.0001	0.029	0.133
				FT cycles	0.05						
VD8	RR	FT cycles, years, PR	FT cycles, years, PR	Constant	−38.664	0.74	−111.843	−111.277	0.0001	0.653	0.582
				PR	−0.004						
				FT cycles	0.049						
				Years	0.021						

Rockfall and meteorological series have been smoothed using a 15-years moving average, Years and Sample Size have been retained with an annual resolution. Selected predictands correspond to initial variables retained in each model after the stepwise selection.

between the latter and rockfall activity. The coefficients of determination range between 0.60 (SG2) and 0.96 (SG5). Finally, based on the AIC and AICc, the most robust models include annual rainfall and years in combination with temperatures (SG3) or freeze-thaw cycles (SG5).

At Valdrôme, coefficients of determination (ranging between 0.42 for VD1-VD2 and 0.74 for VD8) are significantly lower than those computed at Saint-Guillaume (Table 6). VD1-VD2 both include annual precipitation totals and mean temperature. They show a positive correlation between the smoothed rockfall reconstruction and rainfall with increased rockfall frequency occurring during cooler periods. VD3-VD8 are more robust than VD1-VD2, as evidenced by R^2, AIC, and AICc values, but seem more complex. VD3 differs from VD1-VD2 as it includes "years" as an additional variable. Inclusion of the latter—positively correlated with rockfall activity—increases model robustness (r^2 = 0.67), yet surprisingly inverts the correlation with annual rainfall (r = 0.004). In VD4, the variable "years" was replaced by "sample size." PR and SS have been retained as significant regressors as they are positively associated with rockfall records, but mean temperatures were eliminated in the stepwise procedure. By contrast, VD5-VD8 include the annual number of freeze-thaw cycles as potential regressors. Regardless of the variables included in the analyses, a positive correlation is computed between "freeze-thaw cycles" and rockfall activity. If freeze-thaw cycles are combined with "annual rainfall" (VD5) and "sample size" (VD7), the two latter are eliminated during the stepwise selection and "freeze-thaw cycles" are kept as the only explanatory variable. Robustness of models VD5 and VD7 (with r^2 = 0.65 and r^2 = 0.67, respectively) remains comparable to VD3. In VD6-VD8, characterized by the highest R^2, positive correlations with "years" reveal that rockfall activity remains time-dependent. The negative correlation between "annual rainfall" and rockfall frequency observed in model VD8 does not make sense in physical terms. We find that at Valdrôme, none of the proposed models yields completely satisfactory results. From a physical perspective, VD1-VD2 and VD6 appear most convincing in terms of climate-rockfall interactions.

IV Discussion

4.1 Asynchronous evolution of rockfall activity at both sites

Over the last decades, archival sources and direct observations have been used primarily in mountain regions to document the impacts of climate change on rockfall activity. At high-elevation sites, several studies undoubtedly demonstrated that rock faces are experiencing an increase in the frequency and magnitude of rockfall as a result of global warming and the related thawing and degradation of permafrost (Geertsema et al., 2006; Mourey et al., 2019; Ravanel and Deline, 2011; Ravanel et al., 2013). By contrast, at lower elevations, below the lower permafrost limit, Gruner (2004) and Sass and Oberlechner (2012) conclude that the general upward trend in the frequency of rockfall seen at higher altitudes cannot be seen in observational records of low-elevation sites. At the same time, it should be noted that historical data compiled to date in systematic rockfall inventories are even scarcer at low elevations compared to high altitudes and that a very strong focus of research activities has been towards cryosphere environments (Ravanel et al., 2020). Consequently, the role of meteorological variables and climate change on rockfall frequency remains unclear at sites located outside permafrost environments, despite the fact that most rockfall threatening infrastructure indeed originate from slopes located far below permafrost environments (Trappmann and Stoffel, 2013).

To date, a small number of dendrogeomorphic studies has attempted to detect dependencies of rockfall on meteorological conditions (Perret et al., 2006; Schneuwly and Stoffel, 2008b). A tree-ring reconstruction from the Czech Flysch Carpathians (Silhán et al., 2011) suggests that freeze-thaw cycles would be the most relevant trigger of rockfall activity, whereas rainfall seems to be less important at this study site. In the Crimean Mountains, analysis did not allow identification of significant correlation between rockfall activity and annual precipitation

(Silhán et al., 2013). In the Polish Tatra Mountains, Zielonka and Wronska-Walach (2019) evidenced complex relationships between rockfall activity and different meteorological variables (i.e., cumulative precipitation and temperatures in selected months of a year). Whereas these studies clearly point to the potential of dendrogeomorphology to yield continuous time series of rockfall activity with seasonal to yearly resolution spanning up to several centuries (Stoffel, 2006), systematic and in-depth assessments or conclusive results on rockfall–climate relations could not be obtained so far.

According to Trappmann et al. (2013), Silhán et al. (2013), or Trappmann and Stoffel (2015), this lack can be explained partly by artifacts in dendrogeomorphic reconstructions that are related to (1) the continuous reduction in the number, diameter and age of trees impacted by rockfall as one goes back in time (Stoffel et al., 2005a), (2) the decline in the number of potentially recordable GDs (Stoffel and Perret, 2006) as well as (3) the complex detection of old, overhealed scars becoming virtually invisible on the stem surface (Trappmann and Stoffel, 2015).

The study presented here aims at overcoming these limitations by quantifying the potential impacts of meteorological conditions and especially of recent global warming on rockfall activity at two cliffs located well below permafrost environments using a dendrogeomorphic approach. To minimize biases and to assess the robustness of our reconstructions, we (1) mapped all trees within two plots in the calcareous French Prealps, (2) sampled trees and accurately estimated their potential to intercept rockfall over time using highresolution maps and (3) used hourly resolved meteorological time series extracted from the SAFRAN analysis system (1959–2017; Durand et al., 2009a) to characterize the climatic evolution at the study sites. Over the period covered by both datsets, sample depth changed only slightly at Valdrôme (from 175 to 179 trees), but increased more sharply at Saint-Guillaume (from 101 to 179 trees). As a result, the conditional impact probability (CIP) only increased from 0.87 to 0.88 at Valdrôme, whereas interception of rockfall by the sampled trees increased from 42 to 89% between 1959 and 2017 at Saint-Guillaume.

Multidecadal variability in rockfall activity agrees poorly between the two sites, pointing to local drivers of rockfall activity. We do not evidence any significant trend in rockfall activity at Valdrôme, whereas at Saint-Guillaume, and despite CIP correction and detrending of the reconstruction, we find a sharp increase in rockfall activity. The time-dependent increase in rockfall activity at Saint-Guillaume could have two origins and can likely be ascribed to (i) the persistence of biases in the reconstruction, despite CIP correction, or (ii) a warming-induced increase in rockfall activity.

Figure 4 underlines that any conclusion on the reasons for the increasing rockfall activity cannot be given easily. For the period 1946–2012, a diachronic analysis of aerial photographs (Figure 4(a)) provides further evidence for a continuous forest colonization in the upper part of the study site at Saint-Guillaume. Grassy surfaces with individual shrubs are still clearly visible on the 1946 aerial photograph; these surfaces are progressively colonized by an increasingly denser forest since the 1970s. This forest dynamic is confirmed by the age distribution found in the trees sampled (Figure 4(c)). This forest dynamic provides evidence that a climatically induced increase in rockfall activity is unlikely, but instead rather tends to confirm that a bias could remain in the tree-ring reconstruction and be reflective of the massive forest recolonization. A comparable bias has been evidenced in the Queyras massif (French Alps) where a sharp increase in the frequency of tree-ring reconstructed snow avalanches has been undoubtedly attributed to the recolonization of snow avalanche paths with trees following abandonment of grazing (Mainieri et al., 2020b; Zgheib et al., 2022). Figure 4(b) presents the evolution in the number of GDs per tree since 1890 and clearly indicates that trees with ages between 20 and 80 years seem to be more susceptible to record rockfall, which is in line with findings of (Silhán et al., 2013). We can thus reasonably hypothesize that the trends in rockfall activity observed at Saint-Guillaume may result from the over-representation of young trees in the distribution of sampled trees. By contrast, at Valdrôme, the homogeneity of the reforestation plot planted at the turn of the 20th century allows exclusion of a sampling bias

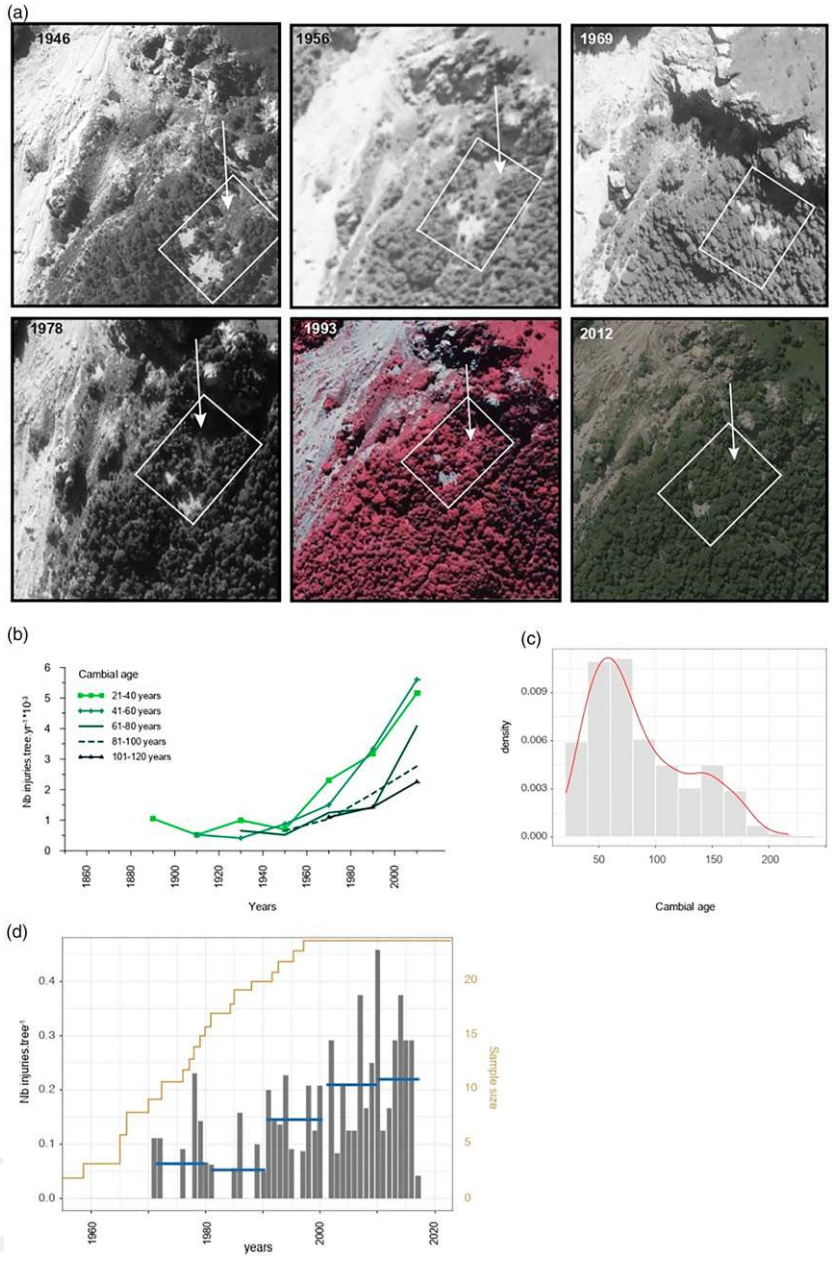

Figure 4. Diachronic evolution of the Saint-Guillaume slope between 1946 and 2012. Aerial photographs of the landslide in (a) 1948 (National Geographic Institute, aerial mission, 1946-07-03-C3136-0151), 1956 (1956-05-07-C3234-0081), 1969 (1969-08-20-C3236-0011), 1978 (1978-09-03-C3136-0021), 1993 (1993-07-27-CN93000014) and 2012 (2012- 06-30-CP12000312). The white rectangle delineates the study site; white arrows indicate areas where forest colonization is obvious. Evolution of the number of GDs per tree over the period 1890–2017 for 20-years class ages (b) and distribution of the cambial ages of sampled trees (c) at Saint-Guillaume. Panel (d) represents the annual (in gray bars) and decadal (horizontal blue line) number of impacts per tree computed for cross-sections of 24 trees cut at the Saint-Guillaume plot. For interpretation of the references to colours in this figure legend, refer to the online version of this article.

(Figure 4(d)), but we cannot completely rule out a possible impact of global warming on rockfall activity.

4.2 Rockfall activity and global warming

Disentangling the respective impacts that methodological biases, forest colonization as well as global warming on rockfall activity is particularly complex at the Saint-Guillaume study site, despite the statistical robustness of the (multiple) regression models were used. The remaining interferences thus considerably limit reliability of the regression models. One therefore should put the validity of the correlations computed between the smoothed rockfall frequency, mean temperature ($r = 0.64$) and freeze-thaw cycles ($r = -0.37$) into question when it comes to assess the period 1959–2017, supposing that increasing mean air temperatures (and the decreasing number freeze-thaw cycles) would increase rockfall activity. This is even more so relevant as a large body of monitoring and to a lesser extent, tree-ring based studies (Amitrano et al., 2012; D'Amato et al., 2016; Frayssines and Hantz, 2006; Imaizumi et al., 2020; Matsuoka and Sakai, 1999; Matsuoka, 2019; Perret et al., 2006) evidenced significant impacts of thermal and freezing stress on rockfall activity.

At Valdrôme, the limited evolution of the forest stand increases our confidence in the reconstruction and, as a corollary, in the rockfall-climate models. VD1-VD2 with the positive correlation between the rockfall reconstruction and annual precipitation as well a negative association with mean temperature are in line with existing literature. Indeed, precipitation (and intense rainfall) were demonstrated to raise water pressure in rock joints or to lead to the lubrification of joints (Matsuoka, 2019). Results obtained at Valdrôme are also in line with findings of D'Amato et al. (2016) based on LiDAR data from the calcareous Chartreuse Massif, located 90 km to the north of the Valdrôme study site. In their study, D'Amato et al. (2016) reported that rockfall activity significantly increased when mean rainfall intensity exceeded 5 mm^{-1}. By contrast, our results differ from several tree-ring reconstructions (Perret et al., 2006; Silhán et al., 2011) where no evidence for positive or negative correlations between rockfall rates and precipitation could be found in the Flysch Carpathians and the Swiss Prealps. Therefore, the absence of a clear trend over the last decades suggests that rockfall activity has not been affected in a significant manner by ongoing climate change. These results should be put in perspective as (1) despite the unusually high resolution of the climatic dataset and the stringency of our reconstruction, the multiple regression models can only account for 42% of the decadal fluctuations observed in rockfall activity at Valdrôme. In other words, some 60% of medium-term rockfall variations are not explained by climatic variables and could be generated by other factors as anthropic or seismic activity (Franco-Ramos et al., 2017; Imaizumi et al., 2020). In addition, VD3 and VD8, characterized by negative correlations between rockfall frequency and precipitation, clearly demonstrate the possibly strong variability of relations between rockfall and climatic fluctuations. Furthermore, (2) tree-ring reconstructions still suffer from limitations in fully capturing process activity (Stoffel and Corona, 2014). Small-magnitude rockfall seem to be more susceptible to global warming (Krautblatter and Moser, 2009) but likely is only poorly captured in tree-ring records due to the limited kinetic energy of small fragments—often insufficient to damage the bark and to disturb woody tissues (cambium). Similarly, the yearly resolution of dendrogeomorphic reconstructions tends to preclude a precise attribution of a given meteorological event (e.g., intense rainfall, freeze-thaw cycles) on rockfall activity as the latter operate at much smaller temporal scales (i.e., a few minutes to a few months). Finally, (3) the 60-years period (i.e., 1959–2017) covered by the SAFRAN reanalysis data probably precludes detection of significant changes in rockfall activity as mean annual air temperature has only risen slightly over the recent decades (from 9°C in 19,591,980 to 9.3°C between 1995 and 2017) and as the number of freeze-thaw cycles has not changed significantly since the 1980's.

V Conclusions and outlook

Over the last two decades, a large body of literature has provided conclusive evidence of relationships between global warming, permafrost thawing and increasing rockfall activity from englaciated alpine cliffs. By contrast, at lower elevations, scarce and

often very incomplete inventories have prevented the identification of any clear impacts of increasing air temperatures on process activity. On forested slopes, various tree-ring based rockfall reconstructions have been developed in mountain regions across the world to overcome the limitations of historical chronicles. In this paper, we compare dendrogeomorphic rockfall reconstructions from two slopes located in the Vercors and Diois massifs (French Prealps). Despite the stringency of the procedure used to sample the trees and to estimate potentially missed events, we do not find synchronous decadal fluctuations between reconstructions that would plead for a regional climate forcing of rockfall activity. At Saint-Guillaume (Vercors massif), and even if impacts of global warming cannot be excluded fully, we conclude that the strong, time-dependent increasing trend observed in rockfall activity would result from a rapid forest colonization observed since 1946 and the overrepresentation of young trees that are more sensitive to rockfall damage (due to their thinner bark). At Valdrôme, the forest plot planted at the beginning of the 20th century evolved only slightly during the period used for analysis (1957–2017). Comparison between the rockfall reconstruction and climatic variables highlight annual precipitation sums and mean air temperatures as the main drivers of rockfall activity. The absence of clear trends in the reconstruction also suggest that climate change would—if at all—only have a limited effect on rockfall activity. Yet, these findings should be interpreted cautiously given the limited robustness of our multiple regression models, the limited increase of temperature since 1959 at the study sites and possible remaining limitations inherent to tree-ring reconstructions. Based on this, we plead for the development of regional rockfall databases coupling historical archives (Coro et al., 2015; Eckert et al., 2020) and tree-ring records that would enable isolation of robust trends that are free from site-dependent dynamics and to compare rockfall activity for periods characterized by very different climatic conditions.

Declaration of conflicting interests

The author(s) declared no potential conflicts of interest with respect to the research, authorship, and/or publication of this article.

Funding

The author(s) disclosed receipt of the following financial support for the research, authorship, and/or publication of this article: This work was supported by the Agence Nationale de la Recherche (Grant No. ANR-15-IDEX-02) and Ministère de l'Écologie, du Développement Durable et de l'Énergie.

ORCID ID

Robin Mainieri https://orcid.org/0000-0001-7184-1876

References

Alestalo J (1971) Dendrochronological interpretation of geomorphic processes. *Fennia - International Journal of Geography* 105(1): 1971.

Allen S and Huggel C (2013) Extremely warm temperatures as a potential cause of recent high mountain rockfall. *Global and Planetary Change* 107:59–69.

Amitrano D, Gruber S and Girard L (2012) Evidence of frostcracking inferred from acoustic emissions in a high-alpine rock-wall. *Earth and Planetary Science Letters* 341–344: 86–93.

André M-F (1997) Holocene rockwall retreat in svalbard: a triple-rate evolution. *Earth Surface Processes and Landforms* 22(5): 423–440.

Bajni G, Camera CAS and Apuani T (2021) Deciphering meteorological influencing factors for alpine rockfalls: a case study in Aosta Valley. *Landslides* 18(10): 3279–3298.

Bakun-Mazor D, Hatzor YH, Glaser SD, et al. (2013) Thermally vs seismically induced block displacements in Masada rock slopes. *International Journal of Rock Mechanics and Mining Sciences* 61: 196–211.

Berti M, Martina MLV, Franceschini S, et al. (2012) Probabilistic rainfall thresholds for landslide occurrence using a bayesian approach. *Journal of Geophysical Research: Earth Surface* 117(F4): 2012.

Birsan M-V, Molnar P, Burlando P, et al. (2005) Streamflow trends in Switzerland. *Journal of Hydrology* 314(1–4): 312–329.

Bovis MJ, Eisbacher GH and Clague JJ (1985) Destructive mass movements in high mountains: hazard and management. *Arctic and Alpine Research* 17(4): 470.

Collins BD and Stock GM (2016) Rockfall triggering by cyclic thermal stressing of exfoliation fractures. *Nature Geoscience* 9(5): 395–400.

Collins BD, Stock GM, Eppes M-C, et al. (2018) Thermal influences on spontaneous rock dome exfoliation. *Nature Communications* 9(1): 762.

Coro D, Galgaro A, Fontana A, et al. (2015) A regional rockfall database: the eastern alps test site. *Environmental Earth Sciences* 74(2): 1731–1742.

Crozier M (2010) Deciphering the effect of climate change on landslide activity: a review. *Geomorphology* 124(3–4): 260–267.

Cruden DM and Varnes DJ (1996) Landslides: investigation and mitigation. Chapter 3 - landslide types and processes. *Transportation Research Board Special Report* 247: 36–75.

D'Amato J, Hantz D, Guerin A, et al. (2016) Influence of meteorological factors on rockfall occurrence in a middle mountain limestone cliff. *Natural Hazards and Earth System Sciences* 16(3): 719–735.

Deline P (2009) Interactions between rock avalanches and glaciers in the Mont Blanc massif during the late holocene. *Quaternary Science Reviews* 28(11–12): 1070–1083.

Deline P, Gardent M, Magnin F, et al. (2012) The morphodynamics of the mont blanc massif in a changing cryosphere: a comprehensive review. *Geografiska Annaler: Series A, Physical Geography* 94(2): 265–283.

Delonca A, Gunzburger Y and Verdel T (2014) Statistical correlation between meteorological and rockfall databases. *Natural Hazards and Earth System Sciences* 14(8): 1953–1964.

Dorren L, Berger F, Jonsson M, et al. (2007) State of the art in rockfall – forest interactions. *Schweizerische Zeitschrift Fur Forstwesen* 158(6): 128–141.

Draebing D and Krautblatter M (2019) The efficacy of frost weathering processes in alpine rockwalls. *Geophysical Research Letters* 46(12): 6516–6524.

Draebing D, Haberkorn A, Krautblatter M, et al. (2017a) Thermal and mechanical responses resulting from spatial and temporal snow cover variability in permafrost rock slopes, steintaelli, swiss alps. *Permafrost and Periglacial Processes* 28(1): 140–157.

Draebing D, Krautblatter M and Hoffmann T (2017b) Thermocryogenic controls of fracture kinematics in permafrost rockwalls. *Geophysical Research Letters* 44(8): 3535–3544.

Dunlop S (2010) *Rockslides in a Changing Climate: Establishing Relationships between Meteorological Conditions and Rockslides in Southwestern Norway for the Purposes of Developing a Hazard Forecast System*. Thesis, Queen's University. https://qspace.library.queensu.ca/handle/1974/5432

Durand Y, Giraud G, Laternser M, et al. (2009a) Reanalysis of 47 years of climate in the French alps (1958–2005): climatology and trends for snow cover. *Journal of Applied Meteorology and Climatology* 48(12): 2487–2512.

Durand Y, Laternser M, Giraud G, et al. (2009b) Reanalysis of 44 yr of climate in the French alps (1958–2002): methodology, model validation, climatology, and trends for air temperature and precipitation. *Journal of Applied Meteorology and Climatology* 48(3): 429–449.

Eckert N, Mainieri R, Bourrier F, et al. (2020) Une base de données évènementielle du risque rocheux dans les Alpes Françaises. *Revue Française de Géotechnique* 3: 163.

Evans S and Degraff J (2002) *Catastrophic Landslides: Effects, Occurrence, and Mechanisms, volume 15 of Reviews in Engineering Geology*. Geological Society of America.

Evans S and Hungr O (1993) The assessment of rockfall hazard at the base of talus slopes. *Canadian Geotechnical Journal* 30(4): 620–636.

Favillier A, Mainieri R, Saez JL, et al. (2017) Dendrogeomorphic assessment of rockfall recurrence intervals at Saint Paul de Varces, western French alps. *Géomorphologie: Relief, Processus, Environnement* 23(2): 11681.

Fischer L, Purves RS, Huggel C, et al. (2012) On the influence of topographic, geological and cryospheric factors on rock avalanches and rockfalls in high-mountain areas. *Natural Hazards and Earth System Sciences* 12(1): 241–254.

Franco-Ramos O, Stoffel M and Vazquez-Selem L (2017) Treering based reconstruction of rockfalls at cofre de perote volcano, Mexico. *Geomorphology* 290: 142–152.

Frayssines M and Hantz D (2006) Failure mechanisms and triggering factors in calcareous cliffs of the subalpine ranges (French Alps). *Engineering Geology* 86(4): 256–270.

Gariano SL and Guzzetti F (2016) Landslides in a changing climate. *Earth-Science Reviews* 162: 227–252.

Geertsema M, Hungr O, Schwab JW, et al. (2006) A large rockslide–debris avalanche in cohesive soil at pink mountain, northeastern British Columbia, Canada. *Engineering Geology* 83(1–3): 64–75.

Giacona F, Eckert N, Corona C, et al. (2021) Upslope migration of snow avalanches in a warming climate. *Proceedings of the National Academy of Sciences* 118(44): 2107306118.

Gruner U (2004) Klima und sturzereignisse in vergangenheit und zukunft. *Bulletin Fur Angewandte Geologie* 12:23–37.

Gunzburger Y, Merrien-Soukatchoff V and Guglielmi Y (2005) Influence of daily surface temperature fluctuations on rock slope stability: case study of the Rochers de Valabres slope (France). *International Journal of Rock Mechanics and Mining Sciences* 42(3): 331–349.

Haeberli W and Beniston M (1998) Climate change and its impacts on glaciers and permafrost in the alps. *Ambio* 27(4): 258–265.

Hale A, Calder E, Loughlin S, et al. (2009) Modelling the lava dome extruded at soufriere` hills volcano, montserrat, August 2005–May 2006. *Journal of Volcanology and Geothermal Research* 187(1–2): 69–84.

Hales TC and Roering JJ (2007) Climatic controls on frost cracking and implications for the evolution of bedrock landscapes. *Journal of Geophysical Research* 112(F2): F02033.

Helsel DR and Hirsch R (1992) Statistical methods in water resources. In *Studies in Environmental Science,* 49, v–vi. Elsevier. doi: 10.1016/S0166-1116(08)71098-7

Hock, R., G. Rasul, C. Adler, B. Cáceres, S. Gruber, Y. Hirabayashi, M. Jackson, A. Kääb, S. Kang, S. Kutuzov, A. Milner, U. Molau, S. Morin, B. Orlove and H. Steltzer, 2019; High Mountain Areas. In: IPCC Special Report on the Ocean and Cryosphere in a Changing Climate [H.-O. Pörtner, D.C. Roberts, V. Masson-Delmotte, P. Zhai, M. Tignor, E. Poloczanska, K. Mintenbeck, A. Alegría, M. Nicolai, A. Okem, J. Petzold, B. Rama, N.M. Weyer (eds.)]. In press

Huggel C (2009) Recent extreme slope failures in glacial environments: effects of thermal perturbation. *Quaternary Science Reviews* 28(11–12): 1119–1130.

Huggel C, Allen S, Deline P, et al. (2012a) Ice thawing, mountains falling-are alpine rock slope failures increasing? *Geology Today* 28(3): 98–104.

Huggel C, Clague JJ and Korup O (2012b) Is climate change responsible for changing landslide activity in high mountains?: climate change and landslides in high mountains. *Earth Surface Processes and Landforms* 37(1): 77–91.

Ilinca V (2009) Rockfall hazard assessment. Case study: lotru valley and olt gorge. *Revista de geomorfologie* 11:101–108.

Imaizumi F, Trappmann D, Matsuoka N, et al. (2020) Interpreting rockfall activity on an outcrop–talus slope system in the southern Japanese Alps using an integrated survey approach. *Geomorphology* 371: 107456.

Keefer DK (2002) Investigating landslides caused by earthquakes – a historical review. *Surveys in Geophysics* 23(6): 473–510.

Korup O (2006) Rock-slope failure and the river long profile. *Geology* 34(1): 45.

Krautblatter M and Moser M (2009) A nonlinear model coupling rockfall and rainfall intensity based on a four year measurement in a high Alpine rock wall (Reintal, German Alps). *Natural Hazards and Earth System Sciences* 9(4): 1425–1432.

Lafaysse M, Morin S, Coleou C, et al. (2013) Towards a new chain of models for avalanche hazard forecasting in French mountain ranges, including low altitude mountains. *International Snow Science Workshop Grenoble – Chamonix Mont-Blanc* 2013: 162–165.

Larson PR (1994) *The Vascular Cambium: Development and Structure*. Heidelberg: Springer Science & Business Media, Springer Series in Wood Science, Springer Verlag.

Luckman BH (1976) Rockfalls and rockfall inventory data: some observations from surprise valley, jasper national park, Canada. *Earth Surface Processes* 1(3): 287–298.

Mainieri R, Lopez-Saez J, Corona C, et al. (2019) Assessment of the recurrence intervals of rockfall through dendrogeomorphology and counting scar approach: a comparative study in a mixed forest stand from the vercors massif (French Alps). *Geomorphology* 340: 160–171.

Mainieri R, Corona C, Chartoire J, et al. (2020a) Dating of rockfall damage in trees yields insights into

meteorological triggers of process activity in the French alps. *Earth Surface Processes and Landforms* 45(10).

Mainieri R, Favillier A, Lopez-Saez J, et al. (2020b) Impacts of land-cover changes on snow avalanche activity in the French alps. *Anthropocene* 30: 100244.

Mainieri R, Corona C, Lopez-Saez J, et al. (2021) Improved tree-ring sampling strategy enhances the detection of key meteorological drivers of rockfall activity. *Catena* 201: 105179.

Malamud BD, Turcotte DL, Guzzetti F, et al. (2004) Landslide inventories and their statistical properties. *Earth Surface Processes and Landforms* 29(6): 687–711.

Matsuoka N (2019) A multi-method monitoring of timing, magnitude and origin of rockfall activity in the Japanese Alps. *Geomorphology* 336: 65–76.

Matsuoka N and Sakai H (1999) Rockfall activity from an alpine cliff during thawing periods. *Geomorphology* 28(3–4): 309–328.

Moreiras SM (2006) Chronology of a probable neotectonic pleistocene rock avalanche, cordon del plata (central andes), mendoza, Argentina. *Quaternary International* 148(1): 138–148.

Morel P, Trappmann D, Corona C, et al. (2015) Defining sample size and sampling strategy for dendrogeomorphic rockfall reconstructions. *Geomorphology* 236: 79–89.

Mourey J, Marcuzzi M, Ravanel L, et al. (2019) Effects of climate change on high alpine mountain environments: evolution of mountaineering routes in the Mont Blanc massif (Western Alps) over half a century. *Arctic, Antarctic, and Alpine Research* 51(1): 176–189.

Moya J, Corominas J, Perez Arcas J, et al. (2010) Tree-ring based assessment of rockfall frequency on talus slopes at sola d'andorra, eastern pyrenees. *Geomorphology* 118(3–4): 393–408.

Muller L (1964) The rock slide in the vajont valley. *Rock Mechanics and Engineering Geology* 2(3–4): 148–212.

Nigrelli G, Fratianni S, Zampollo A, et al. (2018) The altitudinal temperature lapse rates applied to high elevation rockfalls studies in the western European Alps. *Theoretical and Applied Climatology* 131(3–4): 1479–1491.

Noetzli J, Hoelzle M, Haeberli W, et al. (2003) Mountain permafrost and recent Alpine rock-fall events: a GIS-based approach to determine critical factors. In *Permafrost: proceedings of the eighth International Conference on Permafrost*. Lisse: Balkema Publishers.

Paranunzio R, Laio F, Nigrelli G, et al. (2015) A method to reveal climatic variables triggering slope failures at high elevation. *Natural Hazards* 76(2): 1039–1061.

Paranunzio R, Laio F, Chiarle M, et al. (2016) Climate anomalies associated with the occurrence of rockfalls athigh-elevation in the Italian Alps. *Natural Hazards and Earth System Sciences* 16(9): 2085–2106.

Paranunzio R, Chiarle M, Laio F, et al. (2019) New insights in the relation between climate and slope failures at high-elevation sites. *Theoretical and Applied Climatology* 137(3–4): 1765–1784.

Perret S, Stoffel M and Kienholz H (2006) Spatial and temporal rockfall activity in a forest stand in the Swiss Prealps— A dendrogeomorphological case study. *Geomorphology* 74(1–4): 219–231.

Rapp A (1960) Recent development of mountain slopes in karkevagge and surroundings, northern scandinavia. *Geografiska Annaler* 42(2–3): 65–200.

Ravanel L and Deline P (2008) La face ouest des Drus (massif du Mont-Blanc): évolution de l'instabilité d'une paroi rocheuse dans la haute montagne alpine depuis la fin du petit âge glaciaire. *Géomorphologie: Relief, Processus, Environnement* 14(4): 261–272.

Ravanel L and Deline P (2011) Climate influence on rockfalls in high-Alpine steep rockwalls: the north side of the Aiguilles de Chamonix (Mont Blanc massif) since the end of the little ice age. *The Holocene* 21(2):357–365.

Ravanel L, Allignol F, Deline P, et al. (2010). Rock falls in the mont blanc massif in 2007 and 2008. *Landslides*, 7(4):493–501.

Ravanel L, Deline P, Lambiel C, et al. (2013) Instability of a high alpine rock ridge: the lower arête des cosmiques, mont blanc massif, france. *Geografiska Annaler: Series A, Physical Geography* 95(1):51–66.

Ravanel L, Magnin F and Deline P (2017). Impacts of the 2003 and 2015 summer heatwaves on permafrost-affected rock-walls in the Mont Blanc massif. *Science of The Total Environment* 609:132–143.

Ravanel L, Magnin F, Gallach X, et al. (2020) Evolution des parois rocheuses gelées de haute montagne sous forc¸age climatique. *La Météorologie* 111: 034.

Rosser N, Petley D, Lim M, et al. (2005) Terrestrial laser scanning for monitoring the process of hard rock coastal cliff erosion. *Quarterly Journal of Engineering Geology and Hydrogeology* 38(4): 363–375.

Sachs T (1991) *Pattern Formation in Plant Tissues*. Cambridge, MA: Cambridge University Press.

Sass O and Oberlechner M (2012) Is climate change causing increased rockfall frequency in Austria? *Natural Hazards and Earth System Sciences*, 12(11): 3209–3216.

Savi S, Comiti F and Strecker MR (2021) Pronounced increase in slope instability linked to global warming: a case study from the eastern European alps. *Earth Surface Processes and Landforms* 46(7): 1328–1347.

Schneuwly D and Stoffel M (2008a) Spatial analysis of rockfall activity, bounce heights and geomorphic changes over the last 50 years – A case study using dendrogeomorphology. *Geomorphology* 102(3–4): 522–531.

Schneuwly DM and Stoffel M (2008b) *Tree-ring Based Reconstruction of the Seasonal Timing, Major Events and Origin of Rockfall on a Case-Study Slope in the Swiss Alps*. Nat. Hazards Earth Syst. Sci., 2008, Vol. 8, 203–211.

Selby MJ (1993) *Hillslope Materials and Processes*. 2nd edition, Oxford: Oxford University Press,

Silhán K, Brazdil K, Panek T, et al. (2011) Evaluation of meteorological controls of reconstructed rockfall activity in the czech flysch carpathians: evaluation of meteorological controls of rockfall activity. *Earth Surface Processes and Landforms* 36(14): 1898–1909.

Silhán K, Panek T and Hradecky J (2013) Implications of spatial distribution of rockfall reconstructed by dendrogeomorphological methods. *Natural Hazards and Earth System Sciences* 13(7): 1817–1826.

Stahle DW, Fye FK and Therrell MD (2003) Interannual to decadal climate and streamflow variability estimated from tree rings. *In Developments in Quaternary Sciences* 1, 491–504.

Stoffel M (2006) A review of studies dealing with tree rings and rockfall activity: the role of dendrogeomorphology in natural hazard research. *Natural Hazards* 39(1):51–70.

Stoffel M and Corona C (2014) Dendroecological dating of geomorphic disturbance in trees. *Tree-Ring Research* 70(1):3–20.

Stoffel M and Huggel C (2012) Effects of climate change on mass movements in mountain environments. *Progress in Physical Geography: Earth and Environment* 36(3):421–439.

Stoffel M and Perret S (2006) Reconstructing past rockfall activity with tree rings: Some methodological considerations. *Dendrochronologia* 24(1):1–15.

Stoffel M, Lievre I, Monbaron M, et al. (2005a) *Seasonal Timing of Rockfall Activity on a Forested Slope at Taschgufer (Swiss Alps) – a Dendrochronological Approach*. Zeitschrift für Geomorphologie, Berlin Stuttgart, vol. 49(1), 89 –106

Stoffel M, Schneuwly D, Bollschweiler M, et al. (2005b) Analyzing rockfall activity (1600–2002) in a protection forest—a case study using dendrogeomorphology. *Geomorphology* 68(3–4):224–241.

Stoffel M, Wehrli A, Kuhne R, et al. (2006) Assessing the protective effect of mountain forests against rockfall using a 3D simulation model. *Forest Ecology and Management* 225(1–3):113–122.

Stoffel M, Butler DR and Corona C (2013) Mass movements and tree rings: a guide to dendrogeomorphic field sampling and dating. *Geomorphology* 200:106–120.

Stoffel M, Ballesteros Canovas JA, Luckman BH, et al. (2019) Tree-ring correlations suggest links between moderate earthquakes and distant rockfalls in the Patagonian Cordillera. *Scientific Reports* 9(1): 1–9.

Terzaghi K (1962) Stability of steep slopes on hard unweathered rock. *Geotechnique* 12(4):251–270.

Trappmann D and Stoffel M (2013) Counting scars on tree stems to assess rockfall hazards: a low effort approach, but how reliable? *Geomorphology* 180–186.

Trappmann D and Stoffel M (2015) Visual dating of rockfall scars in Larix decidua trees. *Geomorphology* 245:62–72.

Trappmann D, Corona C and Stoffel M (2013) Rolling stones and tree rings: a state of research on dendrogeomorphic reconstructions of rockfall. *Progress in Physical Geography* 37(5):701–716.

Vernay M, Lafaysse M, Hagenmuller P, et al. (2019) The S2M meteorological and snow cover reanalysis in the French mountainous areas (1958 - present). Preprint. https://en.aeris-data.fr/metadata/?865730e8-edeb-4c6b-ae58-80f95166509b

Viani C, Chiarle M, Paranunzio R, et al. (2020) An integrated approach to investigate climate-driven rockfall occurrence in high alpine slopes: the bessanese glacial basin, western Italian Alps. *Journal of Mountain Science* 17(11):2591–2610.

Wieczorek GF and Jager S (1996) Triggering mechanisms and depositional rates of postglacial slope-movement processes in the yosemite valley, California. *Geomorphology* 15(1):17–31.

Zgheib T, Giacona F, Granet-Abisset A-M, et al. (2022) Spatio-temporal variability of avalanche risk in the French Alps. *Regional Environmental Change* 22(1): 8.

Zielonka A and Wronska-Wałach D (2019) Can we distinguish meteorological conditions associated with rockfall activity using dendrochronological analysis? - An example from the tatra mountains (Southern Poland). *Science of The Total Environment* 662: 422–433.